A Transport Equation of the Intermittency Factor for Natural Transition

Ludovic Taguema, Lucas Pascal, François Chedevergne, Julien Cliquet

A Transport Equation of the Intermittency Factor for Natural Transition

Ludovic Taguema*
Airbus Operations SAS, 31060 Toulouse, France

Lucas Pascal† and François Chedevergne ‡
ONERA – University of Toulouse, F-31055 Toulouse, France

Julien Cliquet§
Airbus Operations SAS, 31060 Toulouse, France

In this paper a modified version of the Suzen and Huang [1] transport equation for the intermittency factor γ is proposed. The purpose of this factor is to model the gradual transition from laminar to turbulent flow in a boundary-layer. The model considers longitudinal and wall-normal variations of γ. It has total control, once transition has started, on the advance of turbulence through the weighting of the turbulent eddy viscosity μ_t resulting from a turbulence model. A key parameter of this model is the turbulent spots dimensionless production and propagation rate $\hat{n}\sigma$ which controls the intermittency factor's initial growth and the extend of the transition region. A correlation between $\hat{n}\sigma$ and the free-stream turbulence level Tu is defined for external aerodynamic applications with low Tu. It is validated against experimental data in the boundary-layer code 3C3D [2]. The resulting model is implemented in the RANS solver CODA [3], and coupled to Pascal et al. [4]'s transported transition criteria and Allmaras and Johnson [5]'s turbulence model.

I. Nomenclature

I	=	intermittency function	γ	=	intermittency factor
n	=	spot formation rate	σ	=	spot propagation parameter
N	=	non-dimensional breakdown parameter	$\hat{n}$	=	dimensionless spot formation rate
Tu	=	free-stream turbulence level	k	=	turbulent kinetic energy
ϵ	=	dissipation rate of k	ω	=	specific dissipation rate
ΔRe_{tr}	=	dimensionless transition length	μ	=	molecular viscosity
μ_t	=	turbulent eddy viscosity	ν	=	kinematic viscosity
δ^*	=	boundary-layer displacement thickness	θ	=	boundary-layer momentum thickness
Re_θ	=	momentum-thickness-based Reynolds number	λ_θ	=	Pohlhausen parameter, $(\theta^2/\nu)/(dU/ds)$
$\mathbf{v}$	=	velocity vector	s	=	curvilinear coordinate
x	=	longitudinal coordinate	y	=	span-wise coordinate
z	=	normal coordinate	δ_{ij}	=	Kronecker delta
$\overline{\square}$	=	averaged quantity	$\square_{i,j,k}$	=	Cartesian index notation
$\square_\infty$	=	free-stream variable	$\square_l$	=	laminar variable
$\square_t$	=	turbulent variable	$\square_{tr}$	=	variable at transition point

*Ph.D. student, Airbus Operations SAS, ONERA, Department of Multi-Physics and Energetic, Toulouse Université. ludovic.l.taguema@airbus.com
†Research Scientist, ONERA, Department of Multi-Physics and Energetic
‡Senior Research Scientist, ONERA, Department of Multi-Physics and Energetic
§Dr. Engineer

II. Introduction

In order to produce cleaner and more efficient aircraft, one of the options offered to the aeronautical industry is the reduction of drag forces occurring during flights. Experiments on laminar wing technologies being costly, engineers heavily rely on CFD (computational fluid dynamics), which is an integral component of aircraft development processes. In 2017, during the 52^{th} Paris Air Show, Airbus, Onera and the DLR committed to the joint development of a new RANS solver named CODA (Code Onera DLR Airbus). In that context, it is necessary to provide CODA the ability to correctly simulate the transitional behavior of boundary-layers.

The transition region starts with the appearance of turbulent spots resulting, in the case of natural transition, from the breakdown of Tollmien–Schlichting (TS) waves or of cross-flow instabilities modes. Downstream the transition point, spots grow, propagate and progressively overlap, eventually coalescing into a fully turbulent flow. The intermittency of the flow, defined by the intermittency factor γ, represents the relative fraction of time a given point of the transitional flow is seeing turbulent spots. It is therefore a measure of the progress of the transition from a laminar to a turbulent flow in the boundary-layer. Since Emmons [6] and the discovery of turbulent spots, researchers have focused on the determination of an appropriate distribution for the intermittency and many models have been proposed. While at their beginnings they took the form of algebraic equations [6–8], the use of partial differential equations (PDEs) carrying the intermittency factor has now become a common practice. Basing their research on algebraic expressions of γ [6, 7, 9], Steelant and Dick [10] proposed a transport equation of the intermittency factor that represents the longitudinal distribution of γ in near-wall flows. In the context of free-shear flows Cho and Chung [11] defined a $k-\epsilon-\gamma$ transition PDE system to simulate cross-stream variations of the intermittency. More recently, Suzen and Huang [1] developed a model that results from the blending of Steelant and Dick and Cho and Chung longitudinal and cross-stream distributions of γ.This PDE exhibits the expected behavior both in streamwise and wall-normal directions. Nonetheless, the context of these studies being that of turbomachinery applications, the aforementioned models are only valid for bypass transition.

Langtry and Menter [12] introduced with the $\gamma - Re_\theta$ model a PDE for the intermittency. This PDE is based on phenomenological reasoning as it uses local correlations at Reynolds Average Navier-Stokes (RANS) calculation points for the computation of physical quantities. This use makes it possible to ignore the complex computation of integral quantities. However, local correlation based PDEs are limited in their applications by the range of validity of their correlations.

Thus arises the need for a transport equation of the intermittency factor that can be easily implemented in RANS solvers, which do not rely on locally correlated variables and that is suitable to natural transition.

This paper presents a transport equation for the intermittency factor, derived from the work of Suzen and Huang, modified to agree with natural transition, validated in a boundary-layer solver and implemented in CODA.

Relevant intermittency factor models are first presented in Section III. The modification of Suzen and Huang model is then shown in Section IV and experimental and numerical results are compared in Section V. Finally the integration of the intermittency PDE in CODA and it's coupling to transition criteria and turbulence model is discussed in Section VI.

III. Intermittency models

A. The Suzen and Huang intermittency model

It has been shown [9, 13, 14] that the Reynolds stress tensor of a transitional flow is the sum of a laminar, a turbulent and a laminar-turbulent-interaction contributions:

$$\overline{u'v'} = (1-\gamma)\overline{u'_l v'_l} + \gamma\overline{u'_t v'_t} + \gamma(1-\gamma)(\overline{u_l} - \overline{u_t})(\overline{v_l} - \overline{v_t}) \tag{1}$$

The laminar contribution is related to the variation of instantaneous velocity due to TS waves. The turbulent contribution is directly linked to the presence of turbulent spots in the flow. The interaction contribution results from the difference of mean laminar and turbulent velocities that reflects the interaction of turbulent spots with the laminar flow in transitional boundary-layers. Simon and Stephens [15] showed that in the context of bypass transition for plat plates with zero pressure gradient, the Reynolds stress tensor in the transitional flow can be approximated by its turbulent contribution. They also proved that the intermittency factor can be incorporated in the computation through the weighting of the turbulent eddy viscosity μ_t, as long as the turbulence model can produce fully turbulent flows before the transition point.

Drawing on these findings Suzen and Huang [1] proposed an intermittency model for bypass transition, working in conjunction with Menter's $k-\omega$ SST turbulence model. Indeed the $k-\omega$ SST turbulence model can produce fully turbulent flows in the leading edge of the boundary-layer.

Suzen and Huang model writes:

$$\frac{\partial \rho\gamma}{\partial t} + \frac{\partial \rho u_j \gamma}{\partial x_j} = (1-\gamma)\Big[(1-F)T_0 + F(T_1 - T_2)\Big] + T_3 + D_\gamma \tag{2}$$

T_0 comes from the work of Steelant and Dick and represents the streamwise production of γ. $(T_1 - T_2)$ comes from Cho and Chung and is responsible for the production of γ due to interactions between turbulent spots and the laminar flow, and thus represents the cross-stream distribution of γ in the boundary-layer. F is the blending function that enables the switch from one model to the other. T_3 is a production diffusion-like term from Cho and Chung and D_γ is a diffusion term, also coming from Cho and Chung and modified by Suzen and Huang. All these terms are thereafter presented.

1. Streamwise distribution

T_0 was derived from the algebraic equation of Dhawan and Narasimha [7] that writes:

$$\gamma(s) = \begin{cases} 0 & (s < s_{tr}) \\ 1 - \exp\left(-(s - s_{tr})^2 \frac{n\sigma}{U_{\infty,tr}}\right) & (s \geq s_{tr}) \end{cases} \tag{3}$$

where n is the spot formation rate and σ the dimensionless spot propagation parameter. By differentiating eq. (3) along a streamline s, Steelant and Dick obtained:

$$\frac{\partial \rho\gamma}{\partial t} + \frac{\partial \rho u_j \gamma}{\partial x_j} = (1-\gamma)\rho\sqrt{u_k u_k}\beta(s) \tag{4}$$

with:

$$\beta(s) = \frac{df(s)^2}{ds} \tag{5}$$

Under the hypothesis of concentrated breakdown $f(s)$ is defined as:

$$f(s) = \sqrt{\frac{n\sigma}{U_{\infty,tr}}}(s - s_{tr}) \tag{6}$$

Equation (6) is modified in the work of Suzen and Huang to account for the distributed breakdown hypothesis, characteristic of bypass transition.

T_0 is then defined as :

$$T_0 = \rho\sqrt{u_k u_k}\beta(s) \tag{7}$$

T_0 is based on the universal model of γ from Dhawan and Narasimha and is responsible for the streamwise distribution of the intermittency factor in near-wall flows.

2. Cross-stream distribution

$(T_1 - T_0)$ comes from Cho and Chung PDE source term where:

$$T_1 - T_2 = \gamma\frac{C_1}{k}\tau_{ij}\frac{\partial u_i}{\partial x_j} - \gamma\rho C_2 \frac{k^{3/2}}{\epsilon}\frac{u_i}{\sqrt{u_k u_k}}\frac{\partial u_i}{\partial x_j}\frac{\partial \gamma}{\partial x_j} \tag{8}$$

with $C_1 = 1.60$, $C_2 = 0.16$ and:

$$\tau_{ij} = \mu_t\left[\frac{\partial u_i}{\partial x_j} + \frac{\partial u_j}{\partial x_i} - \frac{2}{3}\frac{\partial u_k}{\partial x_k}\delta_{ij}\right] - \frac{2}{3}\rho k\delta_{ij} \tag{9}$$

T_1 expresses the creation of γ due to the production of turbulent kinetic energy. T_2 represents the destruction of γ due to interactions between the laminar flow and the intermittency field. In eq. (2), $(T_1 - T_2)$ is multiplied by $(1-\gamma)$. $(T_1 - T_2)$ is thus controlled by $\gamma(1-\gamma)$ and therefore tends to 0 for low and high values of γ and is maximal in the middle of the transition region.

$(T_1 - T_2)$ is a source term related to the creation and destruction of γ due to interactions between turbulent spots and the laminar flow. It is responsible for the production of γ in the wall-normal direction.

3. Blending function

T_0 and $(T_1 - T_2)$ are blended with a function F to enable a gradual switch from Steelant and Dick to Cho and Chung model during the transition where:

$$F = \tanh^4 \left[\frac{k/(S\nu)}{200(1-\gamma^{0.1})^{0.3}} \right] \tag{10}$$

With S the magnitude of the strain rate:

$$S = \sqrt{2S_{ij}S_{ij}} \quad \text{where } S_{ij} = \frac{1}{2}\left(\frac{\partial u_i}{\partial x_j} + \frac{\partial u_j}{\partial x_i} \right) \tag{11}$$

When $k/(S\nu) >> 200(1-\gamma^{0.1})^{0.3}$, F tends to 1 and inversely to 0. Therefore, for a given height in the boundary-layer, moving away longitudinally from the transition point increases γ and thus F. The parameter $k/(S\nu)$ increases rapidly with distance away from the wall in the boundary-layer. Thus, for a given longitudinal position in the transition region, moving away from the wall increases $k/(S\nu)$ and in turn F.

The blending function F enables T_0 at the beginning of the transition and near the wall and switches smoothly to $(T_1 - T_2)$ with increased longitudinal and wall-normal distances.

4. Diffusion terms

Two diffusion terms are incorporated in Suzen and Huang PDE: T_3 and D_γ.

$T3$ is a production diffusion-like term developed by Cho and Chung which represents the increase of γ due to inhomogeneities in its gradient:

$$T_3 = C_3 \frac{k^2}{\epsilon} \frac{\partial \gamma}{\partial x_j} \frac{\partial \gamma}{\partial x_j} \tag{12}$$

where $C_3 = 0.15$.

D_γ comes from the work of Libby [16] and corresponds to the diffusion of the intermittency due to differences in relative mean velocities between turbulent spots and the laminar flow:

$$D_\gamma = \frac{\partial}{\partial x_j} \left\{ \gamma(1-\gamma)(\overline{u}_{jl} - \overline{u}_{jt}) \right\} \tag{13}$$

With the help of Lumley [17]'s velocity jump model, Byggstøyl and Kollmann [18] rewrote the previous equation for thin shear flows which is incorporated as such in Cho and Chung model:

$$D_\gamma = \frac{\partial}{\partial x_j} \left\{ (1-\gamma)\nu_t \frac{\partial \gamma}{\partial x_j} \right\} \tag{14}$$

Suzen and Huang extended the above equation to take into account compressibility effects and a new term $\gamma(1-\gamma)\mu$ which considers the diffusion of γ in the viscous-sublayer is added:

$$D_\gamma = \frac{\partial}{\partial x_j} \left\{ \left[\gamma(1-\gamma)\mu + (1-\gamma)\mu_t \right] \frac{\partial \gamma}{\partial x_j} \right\} \tag{15}$$

Suzen and Huang intermittency model was tested against both zero pressure gradient and variable pressure gradient flows with multiple high free-stream turbulence levels. It was able to predict Savill [19]'s ERCOFTAC T3A, T3B, T3C1 and T3C2 experiments.

The streamwise distribution of γ being a function of $n\sigma$, the applicability of the previously discussed model depends on the domain of validity of this product.

B. Correlations for the spot formation rate

As shown previously, T_0 is responsible for the streamwise distribution of γ. T_0 is derived from eq. (3) and depends on $n\sigma/U_{\infty,tr}$. It was shown by Dhawan and Narasimha that whatever the cause of transition, all transition regions define a single universal intermittency distribution. Therefore the $n\sigma/U_{\infty,tr}$ product is the sole governing parameter of the longitudinal distribution of γ for a given height in the boundary-layer.

$n\sigma$ is in $m^{-1}s^{-1}$ and can be expressed under two dimensionless formalisms. Firstly, with the non-dimensional breakdown parameter N from Dhawan and Narasimha and secondly with the dimensionless spot formation rate $\hat{n}$ from Mayle [20]:

$$N = n\sigma\frac{\theta_{tr}^3}{\nu} \quad ; \quad \hat{n} = n\frac{1}{Re_1^2 U_{\infty,tr}} \tag{16}$$

In a thorough study covering a wide range of free-stream turbulence levels Tu (as low as 0.3%) and pressure gradients λ_θ, Gostelow and Walker [21] proposed a correlation for the non-dimensional breakdown parameters N:

$$N = \begin{cases} 0.86\times10^{-3}\exp\left(2.134\,\lambda_{\theta,tr}\ln\left(Tu_{tr}\right) - 59.23\,\lambda_{\theta,tr} - 0.564\ln\left(Tu_{tr}\right)\right) & \lambda_{\theta,tr} \le 0 \\ 0.86\times10^{-3}\exp\left(-0.564\ln\left(Tu_{tr}\right)\right) & \lambda_{\theta,tr} > 0 \end{cases} \tag{17}$$

with the pressure gradient parameter $\lambda_{\theta,tr}$, evaluated at the transition point being equal to:

$$\lambda_{\theta,tr} = \frac{\theta_{tr}^2}{\nu_{tr}}\frac{\mathrm{d}U_{\infty,tr}}{\mathrm{d}s} \tag{18}$$

Using intermittency measurements, Mayle [20] correlated the dimensionless spot formation rate to free-stream turbulence levels at the transition point for turbomachinery applications:

$$\hat{n}\sigma = 1.25\times10^{-11}Tu_{tr}^{7/4} \tag{19}$$

A modified version of this last correlation accounting for gradient pressure effects is used by Suzen and Huang in the expression of T_0.

N and $\hat{n}$ were mainly defined in the context of bypass transition. The applicability of these correlations in conjunction with Suzen and Huang model is not pertinent for natural transition.

IV. Correlation for natural transition

A new transport equation of the intermittency for natural transition is needed: Suzen and Huang longitudinal distribution must be modified to account for the concentrated breakdown hypothesis. A correlation on $n\sigma$ valid for external aerodynamic application is required. It must be easily implemented in CFD solvers and coupled with the AHD transition criteria from Arnal et al. [22] and the ONERA parabolas method [23].

A. Properties and Hypothesis

1. Concentrated breakdown hypothesis

The concentrated breakdown hypothesis states that for flat plate flows with zero pressure gradient, turbulent "spots form at a preferred streamwise location randomly in time and in cross-stream position" [8]. Steelant and Dick modified the term $\beta(s)$ in eq. (4) to account for the distributed breakdown hypothesis specific to bypass transition. It is simply decided to keep the PDE derived from the differentiation of eq. (3) along a stream line s unchanged. T_0 is thus replaced in Suzen and Huang model by:

$$T_0 = 2\rho\frac{n\sigma}{U_{\infty,tr}}(s - s_{tr})\sqrt{u_k u_k} \tag{20}$$

2. On transition length

As shown previously, $n\sigma/U_{\infty,tr}$ is responsible for the longitudinal distribution of γ in the boundary-layer and can thus be linked to the transition length ΔRe_{tr}. ΔRe_{tr} is a dimensionless parameter defined as the difference of Reynolds number between the longitudinal position for which $\gamma = 0.75$ and $\gamma = 0.25$:

$$\Delta Re_{tr} = Re_{s_{\gamma=0.75}} - Re_{s_{\gamma=0.25}} \tag{21}$$

By computing $s_{\gamma=0.75}$ and $s_{\gamma=0.25}$ with eq. (3), the dimensionless transition length can be expressed as a function of Mayle's dimensionless spot formation and propagation rate:

$$\Delta Re_{tr} = \frac{1}{\sqrt{\hat{n}\sigma}}\left[\sqrt{-\ln(0.75)} + \sqrt{-\ln(0.25)}\right] \tag{22}$$

The transition length ΔRe_{tr} at a given boundary-layer height is thus entirely controlled by the dimensionless spot formation and propagation rates $\hat{n}\sigma$.

In a series of experiments over a flat plate with zero pressure gradient, Schubauer and Skramstad [24] studied the impact of free-stream turbulence levels on transition. Their results, presented in fig. 1, show that with decreasing levels of free-stream turbulence, the transition onset is moved to higher values of Re_x all the while the transition length ΔRe_{tr} stays constant.

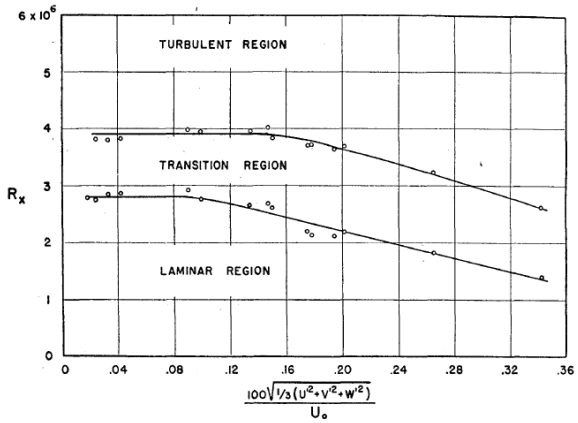

Fig. 1 Effect of levels of free-stream turbulence on the start of transition and on the transition length. Flat plate, zero pressure (Schubauer and Skramstad [24]).

In a study on the effect of free-stream turbulence levels on transition, Fransson et al. [25] observed that decreasing levels of Tu were linked to decreasing rate of spot production which were correlated to increasing transition lengths. Nonetheless, in a boundary-layer, one can expect each start of transition to eventually generate a fully turbulent flow downstream the transition point.

The possibility that there may exist a maximum transition length which is independent of free-stream turbulence levels when Tu is bellow a threshold will be thereafter investigated. $\hat{n}\sigma$ behavior with respect to Tu will hence be examined for the natural transition of 2D flows over a flat plate with zero pressure gradient.

B. Experimental determination of the intermittency

1. Experimental data

In order to investigate $n\sigma$ for natural transition an experimental study of the intermittency of the flow over a flat plate is performed. Two sets of experimental data are used. They are the results of experiments over a flat plate in ONERA TRIN 2 subsonic wind tunnel, under local atmospheric conditions.

The first data-set named $data - set1$ is made of 15 experiments which come from a study by Methel et al. [26] on the effects of two-dimensional positive surface defects on the laminar–turbulent transition of a sucked boundary-layer. The second set of data, named $data - set2$, is composed of 22 experiments resulting from a study by Ducaffy et al. [27] on the effects of surface roughness on the laminar-turbulent transition of a 2D incompressible boundary-layer.

In all 37 experiments, a flat plate is covering the entire width of a test section and its leading edge geometry is designed to have a pressure coefficient C_p null. For Methel et al. the maximum free-stream turbulence was found to be below 0.13% for an operating Reynolds number of 2.6×10^6 m^{-1}. In these conditions, the baseline flow at which all data were acquired is of approximately 40m.s^{-1}. Three suction panels which could be covered were tested during the study. These suction panels were categorized based on their porosity p. The experiments from Methel et al. used in this

paper were performed with no suction and with panels of porosity equal to 0%, 0.26% and 1.34%. All longitudinal measurement were made at a constant boundary-layer height of 300µm which was found to be the height for which the maximum amplitude of the TS wave eigenfunction was obtained.

Ducaffy et al. reported free-stream turbulence levels below 0.04% for operating Reynolds numbers ranging from 2.8 to 4.1×10^6 m^{-1} corresponding to free-stream velocities between 42 and 66m.s^{-1}. Longitudinal measurements were made at a constant wall-distance of 600µm, which corresponds to a distance to the wall which is low enough to always stay in the boundary-layer and high enough not to be in regions where velocity gradients are too important. All measurements from Ducaffy et al. thereafter studied were made over a smooth plate without added roughnesses.
A summary of experimental settings is shown in table 1:

		$data-set1$	$data-set2$
Re	[m^{-1}]	2.6×10^6	$2.6 - 4.1 \times 10^6$
U_∞	[m.s^{-1}]	40.0	44.0 - 66.0
Tu	[%]	0.13	0.04
y	[µm]	300	600

Table 1 Experimental conditions

2. Intermittency Measurements

In this section the process used to extract the intermittency of the flow from longitudinal instantaneous velocities along the flat plate is presented. One experiment from each data-set is used as an example.

The intermittency of the flow at a given boundary-layer height is calculated with the newly developed "rational method for determining intermittency in the transitional boundary-layer" by Veerasamy and Atkin [28]. The idea behind this new method is to define a singular threshold value Th for counting the intermittency based on the magnitude of the maximal laminar perturbation in the boundary-layer. This maximal laminar perturbation is expected to be found at the transition point x_{tr}. This point, according to Bertelrud and Anders [29], should correspond to the streamwise location for which the skewness S of the instantaneous velocity is at its maximum. Due to non-continuous longitudinal measurements, the point x_0 for which S is maximal may not be equal to x_{tr}. The signal skewness, shown in fig. 2, is defined by Veerasamy and Atkin as:

$$S(x) = \frac{\overline{u(x)^3}}{u(x)^3_{rms}} = \frac{1}{n} \frac{\sum_i u(x)_i^3}{\left(\sqrt{\frac{1}{n}\sum_i u(x)_i^2}\right)^3} \tag{23}$$

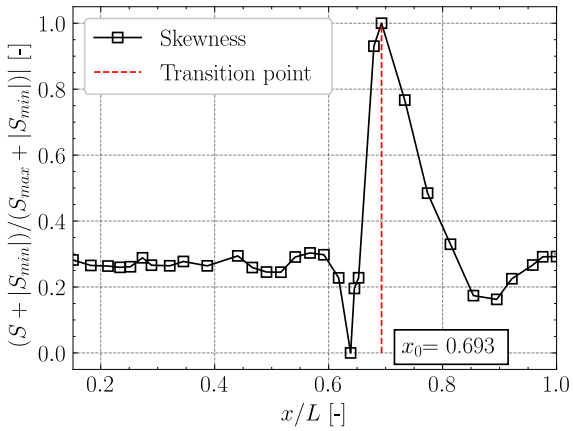

Fig. 2 Skewness of the signal. $data-set1$**.**

At the point x_0 for which the skewness of the signal is maximal, the instantaneous velocity signal is sensitised to high frequencies by squaring its second derivative:

$$D(t)_{x_0} = \left(\frac{\partial^2 u(x_0, t)}{\partial t^2} \right)^2 \tag{24}$$

The set of times corresponding to high frequencies T_{hf} in $D(t)_{x_0}$ is defined as:

$$T_{hf} = \left\{ [t_{i-3}, t_{i+3}] \quad , \quad \forall t_i \in D(t)_{x_0} \quad | \quad D(t_i)_{x_0} > 2D(t)_{x_0,rms} \right\} \tag{25}$$

where the time interval around $t_{i\pm3}$ is here to incorporate turbulent dropouts and tailing signal to the set of turbulent perturbations times.

As shown in shown in fig. 3, Veerasamy and Atkin subtracted the sensitised signal related to turbulent perturbations in T_{hf} from $D(t)_{x_0}$ (gray curve) to obtain the laminar perturbation $D(t)_{x_0,L}$ (red curve). The threshold on laminar perturbation (green line) is then defined as the root mean square of the laminar sensitised signal at x_0:

$$Th = D(t)_{x_0,L,rms} \tag{26}$$

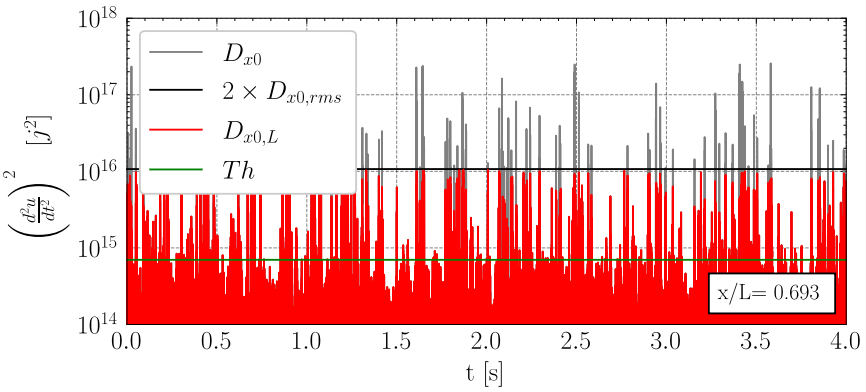

Fig. 3 Determination of the threshold value Th for counting the intermittency. $data - set1$**.**

In order to obtain the intermittency, the sensitised signal $D(t)_x$ is first smoothed with a moving-average window of 7 times the sampling rate, at each streamwise measurement point. It is then then compared to the threshold Th. It comes naturally that the intermittency function and the intermittency factor are:

$$I(t)_x = \begin{cases} 0 & \text{if } mD(t)_x < Th \\ 1 & \text{if } mD(t)_x \geq Th \end{cases} \qquad \gamma_x = \frac{1}{n} \sum_{t_i=0}^{t_i=n} I(t_i)_x \tag{27}$$

with $mD(t)_x$ the moving-average value of $D(t)_x$.

I and γ are easily identified in fig. 4. $I(t)_x$ equals 1 every time $mD(t)_x$ is red and 0 otherwise. γ is the ratio of all times for which $mD(t)_x$ is red over the total measurement duration of $mD(t)_x$.

The resulting intermittency factor for experiments in $data - set1$ and $data - set2$ can be seen in fig. 5

3. Intermittency Post-processing

Veerasamy and Atkin applied their algorithm for the determination of γ to signals taken at $y/\delta^* = 0.5$, with δ^* the displacement thickness. The value of this ratio was chosen because Matsubara et al. [30] showed that wall-normal distribution of γ is constant as long as $y \leq \delta^*$. The previously introduced data-sets present measurement heights that are constant. They are of 300µm for $data - set1$ and 600µm for $data - set2$.

As δ^* decreases with increasing Reynolds number, a single computation of the displacement thickness for a fully laminar and a fully turbulent flow at $Re = 4.1 \times 10^6 \text{m}^{-1}$ is undertaken with 3C3D, a boundary-layer solver from ONERA. In fig. 6, y/δ^* resulting from the aforementioned computation is plotted, with $y = 600$µm. The unit Reynolds number and the measurement height y here taken are the highest of all present in the different experiments. Consequently all y/δ^* extracted from the 37 experiments would be plotted below the red curve in fig. 6.

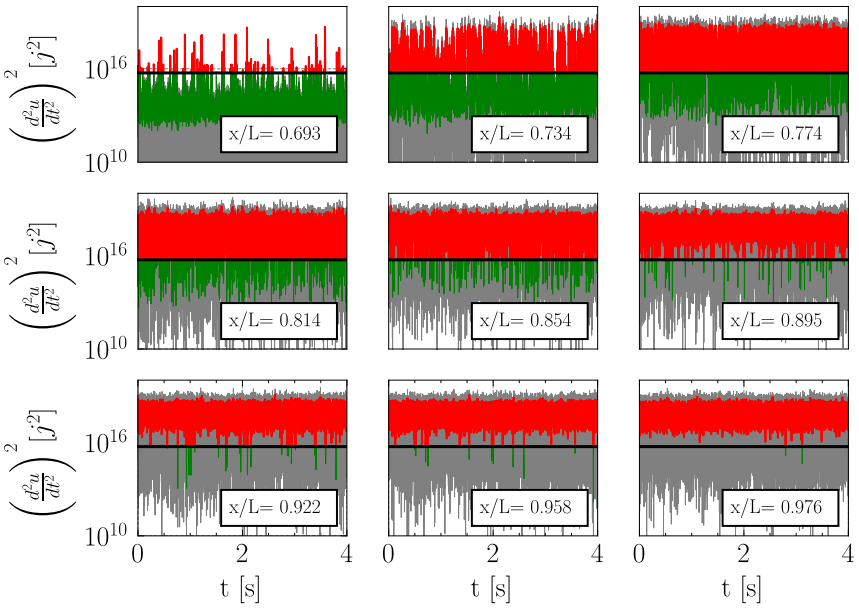

Fig. 4 Experimental determination of γ. In gray, the sensitised velocity fluctuation at given measurement points. In green, the moving average of $D(t)_x$ $mD(t)_x$ at times for which $mD(t)_x$ is below the threshold Th. In in red $mD(t)_x$ at time for which it is higher than the threshold. $data - set1$.

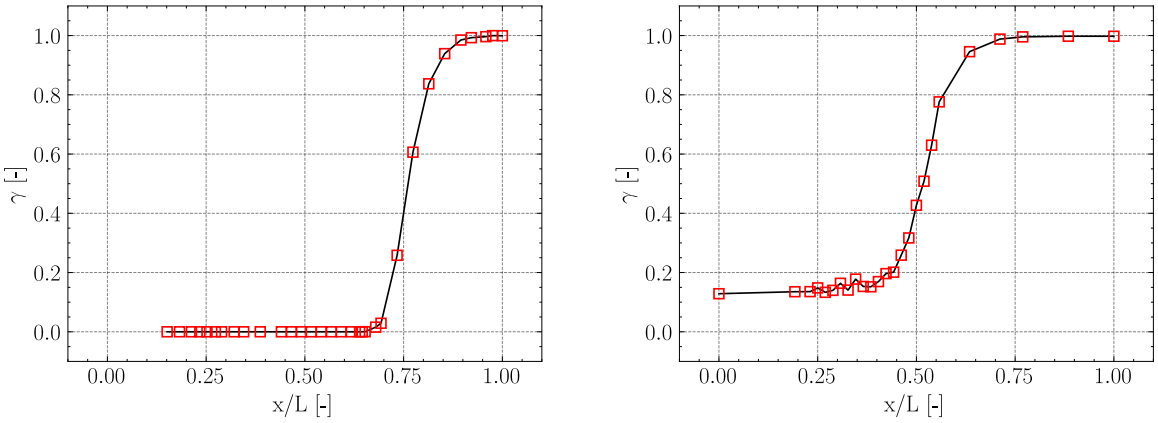

(a) $data - set1$ (b) $data - set2$

Fig. 5 Experimental γ obtained with Veerasamy and Atkin algorithm.

Therefore, it is certain that measurements taken in the transition region (usually starting at $x/L > 0.3$) were all sampled at a height for which $y \leq \delta^*$. Measurement points in the laminar regions, especially for experiments in $data - set2$ are likely to present a y/δ^* ratio higher than one.

The intermittency distribution for the $data - set2$ experiment presented in fig. 5 is not ranging from 0.0 to 1.0 but from around 0.2 to 1.0. Contrary to Veerasamy and Atkin, the present experiments were made at a constant boundary-layer height and so at a non-constant y/δ^*. Hence in the laminar region, most of $data - set2$ measurements were taken at a height y for which y/δ^* is higher than 1.0. TS waves amplitude being function of y/δ^*, the magnitude of the laminar perturbation is less than what it would have been if measured at a lower y/δ^* ratio. Consequently, Veerasamy and Atkin algorithm produces values of Th that are lower than what would have been obtained at lower measurement heights. Hence, the lower threshold produces non-zero γ in the laminar region.

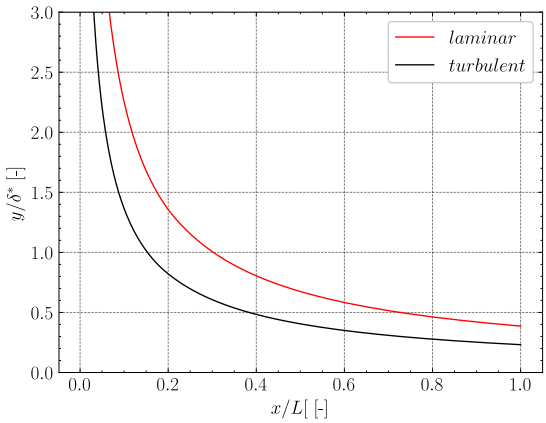

Fig. 6 y/δ^* **for fully laminar and fully turbulent flows over a flat plate.** $y = 600\mu$**m,** $Re = 4.0 \times 10^6$ **m**$^{-1}$**, 3C3D.**

As shown in fig. 6 a ratio of y/δ^* lower than one is to be expected in the transition region. It means that in that region, longitudinal measurements of γ are all made at heights for which γ is maximal. According to Dhawan and Narasimha the longitudinal distribution of γ is universal. Therefore, it is possible, starting from data points in the transitional and turbulent regions, to recreate the laminar and the initial growth of the experimental intermittency distribution that γ would present if measured at a height for which $y \leq \delta^*$ and with y/δ^* constant.

The distribution that γ would follow if measurement points were made at that height can be found by determining the transition point x_{tr} that would enable an intermittency distribution starting in x_{tr} to fit the experimental data in the transitional and turbulent regions. For concentrated breakdown, one can define a function $F(\gamma) = \sqrt{-\ln(1-\gamma)}$ (see Narasimha [8]) which behaves linearly past the transition point. This linear behavior has a slope that is directly linked to the distribution of gamma and that is not related to measurement heights.

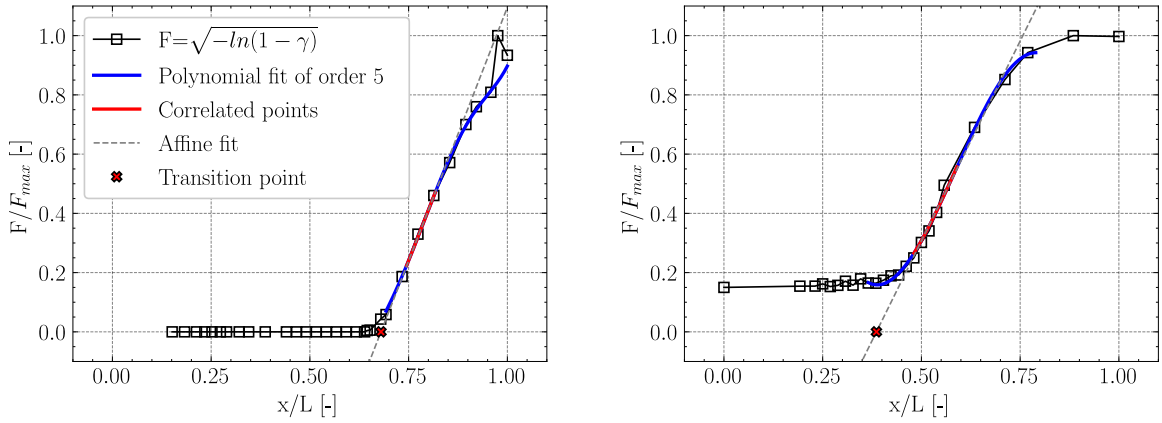

(a) $data - set1$ (b) $data - set2$

Fig. 7 Determination of the transition point.

By fitting the affine part of the function F and finding the point for which this affine fit cut the line $F = 0$, one can determine the point for which transition would occur for an intermittency distribution at an height such that $y \leq \delta^*$ and with y/δ^* constant.

The function F is computed from the experimental intermittency factor. The affine part of F is smoothed with the help of a polynomial fit of order 5, named $P5$. It was found to best capture the initial slow growth, the affine behavior and the saturation of F for all experiments. $P5$ is itself fitted with an affine fit, named $P1$. This fit is performed on values of $P5$ ranging from 0.656 to 1.337 which correspond to intermittencies of 0.35 and 0.85. This way, the affine fit is only applied to the linear part of $P5$ which corresponds to the linear growth of F. The transition point x_{tr} corresponding to a full distribution of γ is found at the intersection of $P1$ and $F = 0$. The application of this process is shown in fig. 7.

It can be seen that for the $data - set1$ experiment which already present a full distribution of γ, x_{tr} corresponds to an abscissa of F for which its linear growth is starting. For the experiment in $data - set2$, where γ and F are not zero in the laminar region, this technique allow the finding of a transition point x_{tr}, upstream x_0 which would belong to the function F such that $y \leq \delta^*$ and and with y/δ^* constant.

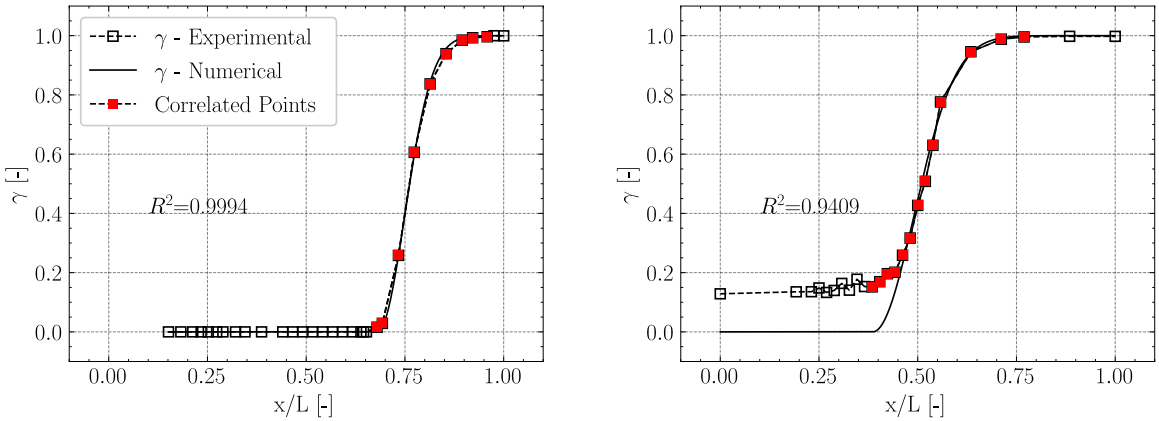

(a) $data - set1$ (b) $data - set2$

Fig. 8 Intermittency factor extracted from experimental data and fitted to Narasimha equation.

With the newly computed transition point x_{tr}, Dhawan and Narasimha's Equation (3) is used to fit the experimental data using a non-linear least square method. The fit is performed on values of γ for which $x > x_{tr}$. The resulting numerical γ can be seen in fig. 8. The coefficient of determination R^2 is computed. For the experiment in $data - set1$, an almost perfect fit is obtained. It once more proves that the streamwise distribution of γ follows the behavior predicted by Narasimha. For the experiment in $data - set2$ a perfect fit for values of the intermittency higher than 0.2 is observed. It can be seen that the numerical intermittency possesses a full distribution that matches the experimental γ past $\gamma = 0.2$. The R^2 is here lower than for the experiment in $data - set1$ as the fit includes data of γ in its initial growth below 0.2. It can nonetheless be concluded that the method enables the finding of full distributions of γ.

V. Validation of the model and discussion

The process presented in section IV.B.2 and IV.B.3 is reproduced for the 37 streamwise measurements at our disposal. Numerical γ resulting from Dhawan and Narasimha's equation fit are retrieved. They are algebraic equations from which the term $n\sigma$ can directly be extracted.

A. Correlation of $\hat{n}\sigma$

In order to compare the product of the turbulent spot production per unit length in the span-wise direction with the dimensionless spot propagation parameter between multiple experiments, the dimensionless quantity $\hat{n}\sigma$ introduced by Mayle is used.

The value of $\hat{n}\sigma$ is extracted from every experiments. First, the impact of surface porosity for experiments in $data - set1$ must be analyzed.

The distribution of $\hat{n}\sigma$ for experiments in $data - set1$ is presented in fig. 9. Every square point is colored based on the value of its R^2, and the percentage of porosity is underlined by different colored circles. High porosity experiments (red circle) present values of $\hat{n}\sigma$ higher than those from no porosity experiment (green circle). Lower percentage of porosity are not related to specific values of $\hat{n}\sigma$ as no specific relation can be found between low porosity and no porosity experiments. Experiments with high porosity or with R^2 lower than 0.95 are discarded.

Due to experimental values of γ that are not zero in the laminar region for experiments in $data - set2$, coefficients of determination R^2 tend to be lower than for data in $data - set1$. The distribution of $data - set2$ $\hat{n}\sigma$ is presented is fig. 10. Experiments with R^2 lower than 0.85 are discarded.

The resulting averaged value of $\hat{n}\sigma$ is found to be equal to:

$$\hat{n}\sigma = 1.46 \times 10^{-11} \tag{28}$$

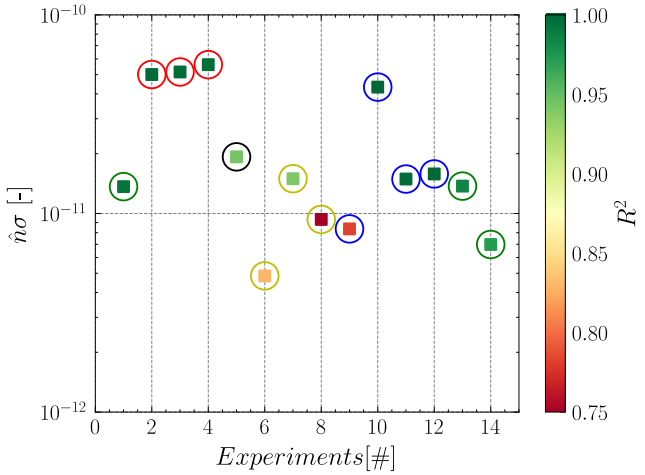

Fig. 9 Distribution of $\hat{n}\sigma$ for experiments in $data - set1$. Squares color: R^2. Circles: Green - p=0%, Yellow - p=0.26% with tape, Blue - p=0.26%, Black - p=1.34% with tape, Red - p=1.34%.

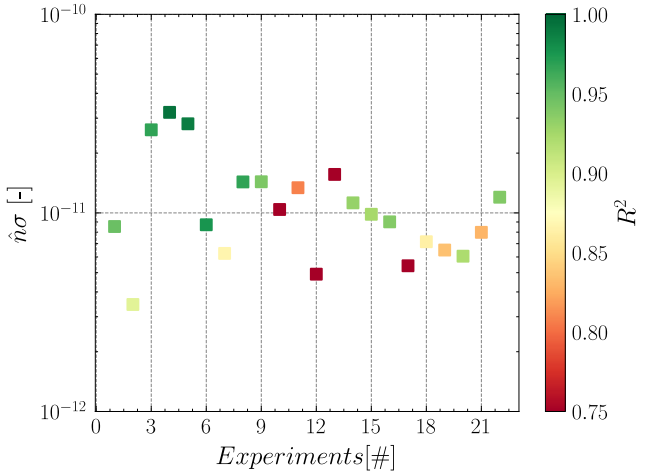

Fig. 10 Distribution of $\hat{n}\sigma$ for experiments in $data - set2$.

B. Validation of the model

Suzen and Huang intermittency equation is implemented into 3C3D [2], a boundary-layer solver from ONERA. It is validated against ERCOFTAC T3A and Suzen and Huang own results as seen in fig. 11.

An excellent agreement is obtained between the data of Suzen and Huang and those obtained from the $k - \omega - \gamma$ SST model implemented in 3C3D. Indeed The two C_f curves are perfectly superimposed.

$\hat{n}\sigma$ is added to the modified expression of T_0 presented in eq. (20) such that:

$$T_0 = 2\rho\hat{n}\sigma Re_1^2(s - s_{tr})\sqrt{u_k u_k} \tag{29}$$

$(T_1 - T_2)$ as well as the diffusion terms are switched off to validate the longitudinal distribution of γ resulting from the modified T_0.

The 37 previously described experiments are simulated with 3C3D. The free-stream velocity, the free-stream turbulence intensity, the unit Reynolds number, and the transition location are imposed in the boundary-layer code. $\hat{n}\sigma$ is set at 1.46×10^{-11} and Suzen and Huang modified model is used in conjunction with the $k - \omega$ SST turbulence model. Figure 12 shows a comparison between experimental γ, numerically fitted γ, and γ resulting from the 3C3D computation.

A very good agreement is found between the different experimental distributions of γ and their corresponding simulation in 3C3D for experiments in $data - set1$. This agreement is less good for experiments in $data - set2$. It is

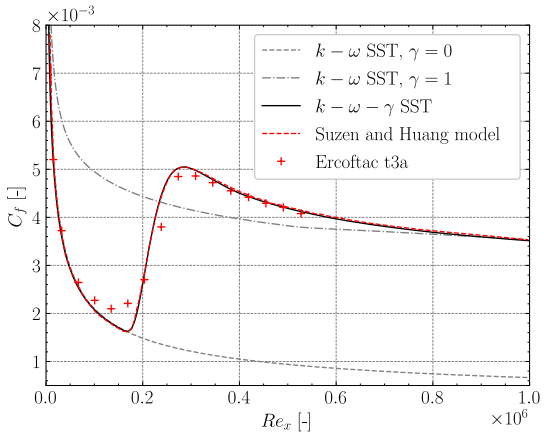

Fig. 11 Validation of Suzen and Huang model's implementation coupled to $k-\omega$ SST in 3C3D.

believed the measurement height, and the resulting post-processing aimed at correcting for the high y/δ^*, introduces error in the measurement of γ and is thus responsible for the distribution of $\hat{n}\sigma$.

However, while experiments in $data-set1$ present free-stream turbulence levels two times higher than experiments in $data-set2$, no specific distribution of $\hat{n}\sigma$ can be found to be correlated with Tu. Indeed, $\hat{n}\sigma$ values from $data-set2$ are found to distributed around those of $data-set1$.

It thus comes that below a certain threshold for Tu, the transition length is not related to free-stream turbulence intensity, and the dimensionless quantity $\hat{n}\sigma$ can be found to be constant with respect to Tu.

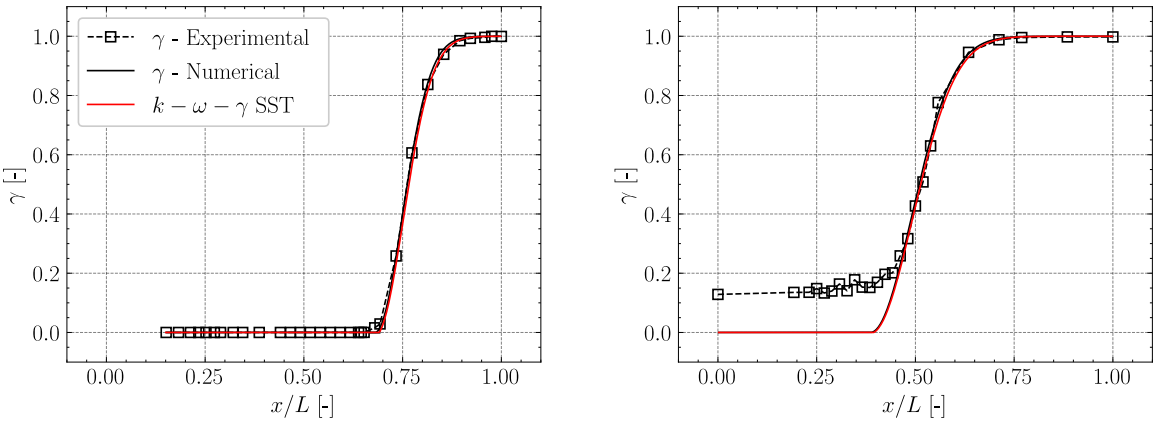

(a) $data-set1$ (b) $data-set2$

Fig. 12 Experimental, numerical and simulated intermittency factor with $\hat{n}\sigma = 1.46 \times 10^{-11}$.

VI. Integration and coupling of the intermittency factor in the RANS solver CODA

The next step of this study consists in the integration of the modified intermittency model into the RANS solver CODA and its validation on a simple test case. To the best of our knowledge, it is the first time this model has been implemented in a RANS solver as Suzen and Huang only implemented their intermittency factor PDE in a boundary-layer solver.

A. Integration and coupling of the intermittency factor

CODA is an unstructured finite volume compressible flow solver aimed at industrial aerodynamic applications. It has been thoroughly described by Leicht et al. in these two papers: [3], [31].

In this solver, under the RANS formulation, the previously derived intermittency factor model was coupled to the Navier-Stokes equations, to Pascal et al. [4]'s transported transition criteria and to the modified version [5] of the Spalart and Allmaras [32]'s one-equation turbulence model. The resulting set of equations reads:

$$\partial_t \mathbf{u} + \nabla \cdot (\mathbf{F}_c(\mathbf{u}) - \mathbf{F}_d(\mathbf{u}, \nabla\mathbf{u})) = \mathbf{S}(\mathbf{u}, \nabla\mathbf{u}) \tag{30}$$

where the vector $\mathbf{u}$ represents the following conservative variables:

$$\mathbf{u} = \left[\underbrace{\rho;\quad \rho\mathbf{v}^T;\quad \rho E;}_{\textit{Mean-flow}} \quad \overbrace{\rho\widetilde{\nu}}^{\text{Turbulence}} \quad ; \quad \underbrace{\rho\widetilde{Re}_{\theta,cr};\quad \rho\widetilde{\bar{\Lambda}_2};\quad \rho\widetilde{s_{cr}};\quad \rho\widetilde{s_{tr}};}_{\text{Transition}} \quad \overbrace{\rho\gamma}^{\text{Intermittency}} \right]^T \tag{31}$$

with ρ being the density, $\mathbf{v}$ the velocity vector, E the specific total energy, $\widetilde{\nu}$ the modified eddy viscosity, $\widetilde{Re}_{\theta,cr}$ the critical momentum thickness based Reynolds number, $\widetilde{\bar{\Lambda}_2}$ the integral along a streamline s of the Pohlhausen parameter, $\widetilde{s_{cr}}$ the curvilinear abscissa measured from the critical point, $\widetilde{s_{tr}}$ the curvilinear abscissa measured from the transition point, and γ the intermittency factor.

$\mathbf{F}_c(\mathbf{u})$ and $\mathbf{F}_d(\mathbf{u}, \nabla\mathbf{u})$ are respectively the convective and diffusive fluxes of $\mathbf{u}$ and of its gradient. $\mathbf{S}(\mathbf{u}, \nabla\mathbf{u})$ is the source term vector. It acts on conservation equations for all but mean-flow variables. Mean-flow, transition and turbulence equations are detailed in section VIII.

Boundary-layer quantities are calculated from the mean-flow and used in the stability based transition model to evaluate transition criteria along streamlines. Once the transition is found, the curvilinear abscissa measured from the transition point is retrieved. $\widetilde{s_{tr}}$ is in turn injected in the intermittency model where the distance to the transition point is required. The resulting intermittency factor γ weights the turbulent eddy viscosity μ_t obtained from the turbulence model. The effective eddy viscosity, defined as $\mu_{eff} = \gamma\mu_t$, is integrated in the diffusive part of mean-flow equations (see section VIII.A). It however does not appear in the production, destruction or diffusion term of the turbulence model. Thus the turbulence model enables the solution of μ_t to display fully turbulent features before the transition location, as recommended by Suzen and Huang. It thus gives the intermittency factor the full control on the transition progress.

B. Validation and Discussion

To validate the implementation and coupling of mean-flow, transition, intermittency and turbulence models in CODA, a preliminary study was carried out.

This study consists in the simulation of the flow along a flat plate without pressure gradient, at Mach number $Ma = 0.3$, and at unitary Reynolds Number $Re = 1.925 \times 10^6$. The body reference length is 1 unit. A structured mesh with 33282 nodes was used. Figure 13 shows the layout of the flat-plate grid, along with the boundary conditions.

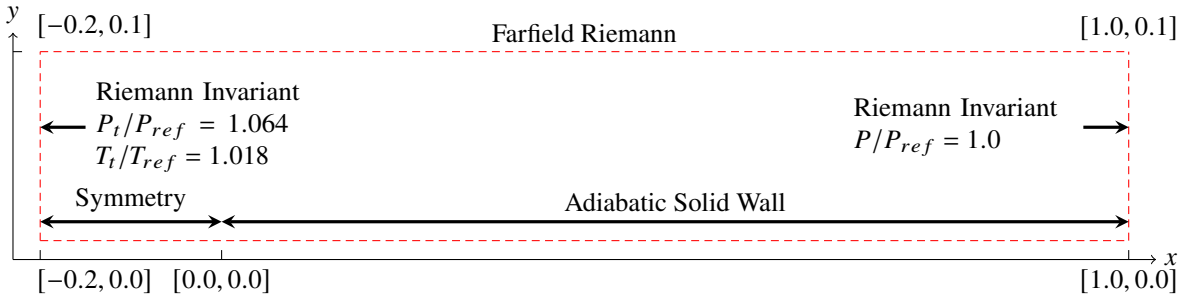

Fig. 13 Flat-plate boundary conditions

The free-stream intensity at the leading edge is 0.1% and the viscosity ratio is $\mu_t/\mu = 4.0$ for the Spalart and Allmaras turbulence model. A linearized implicit Euler method is used in conjunction with a finite volume discretization. Integral quantities required in the transition model are computed every 10 iterations, and drag coefficients every iterations.

The residual of $\mathbf{u}$'s variables, which is the $L2$ norm of the initial residue, can be seen in Figure 14a. The drag convergence is detailed in Figure 14b. Before the transition point is found by the transition model, $\widetilde{s_{tr}}$ and γ's residuals do not exist, γ is set to 0 everywhere and drag coefficients converge toward laminar values. With our current numerical settings, transition is found after around 250 iterations. From that iteration onward, we observe a quick drag convergence, and a steep decrease of every residual.

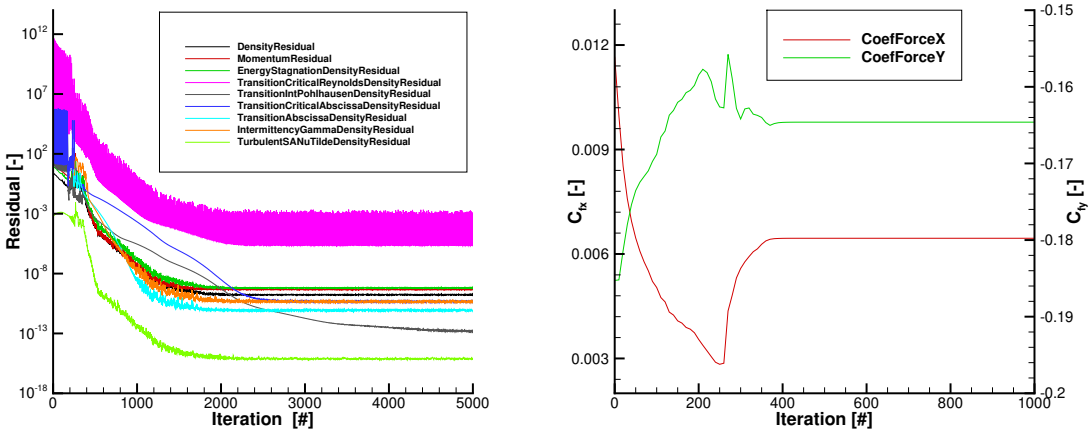

(a) Residuals

(b) Drag Convergence

Fig. 14 Residuals and Convergence.

The transition model found the transition onset at $x_{tr} = 0.639$. The behavior of the intermittency factor and other relevant variables past this point is discussed thereafter.

$T0$ controls the initial production of the intermittency factor. Its normal variations seen in Figure 15a are due to the presence of the norm of the velocity in its definition. Its longitudinal linear growth is proportional to $\widetilde{s_{tr}}$.

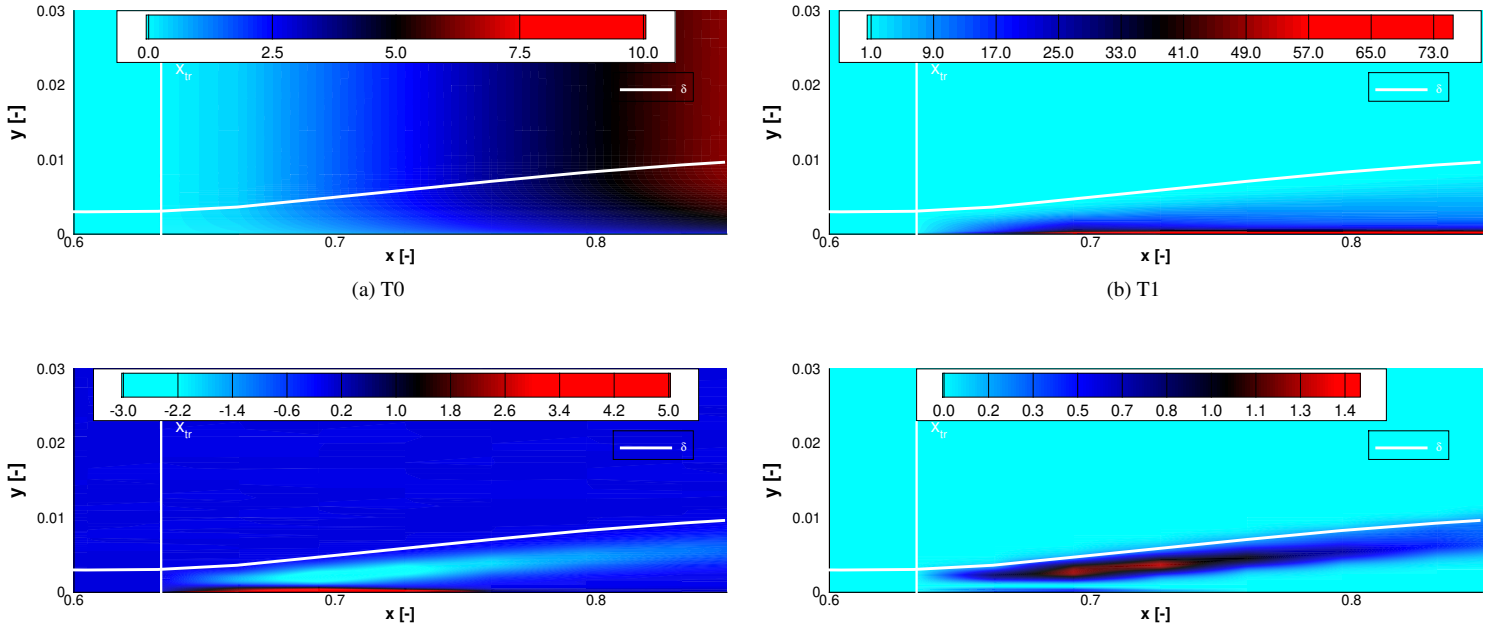

(a) T0

(b) T1

(c) T2

(d) T3

Fig. 15 Intermittency factor source terms.

$T1$ and $T2$ are shown in Figure 15b and Figure 15c. $T1$ is close to 0 everywhere but near the the wall. Indeed, $T1$ is function of P_k, a turbulent kinetic energy production-like term. It thus produces intermittency in regions where the production of k is important. $T2$ relates velocity gradients to intermittency gradients and thus represents the production and destruction of γ due the interaction between turbulent spots and the laminar flow in the boundary-layer. It has a destructive effect at the wall, where $T2$ is positive, and a productive effect in the boundary-layer, away from the wall, where $T2$ is negative.

$T3$, which is shown in Figure 15d, is null everywhere but at the beginning of the transition and near the boundary-layer edge, where intermittency gradients are important.

The blending function F represented in Figure 16 shows that $T0$ is activated at the beginning of the transition and at the wall. $(T1 - T2)$ is activated in the boundary-layer, with increasing distance away from the transition point and from the wall. The blending function defined by Suzen and Huang is only valid inside the boundary layer. We thus force $F = 1.0$ outside of the boundary-layer.

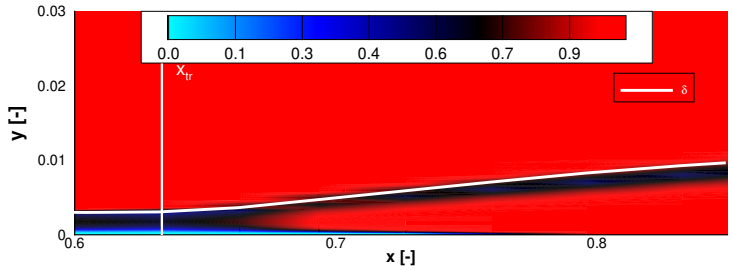

Fig. 16 Blending function.

The resulting intermittency can be seen in Figure 17. Its is null before the transition point and from there, smoothly increases with longitudinal distance away from x_{tr}.

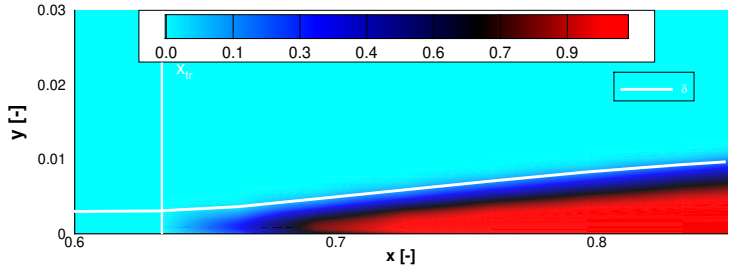

Fig. 17 Intermittency factor γ.

The behavior of γ in the wall normal direction is detailed in Figure 18. For a given longitudinal position, the maximum of γ is found close to the wall, at about $y/\delta^* = 1$.

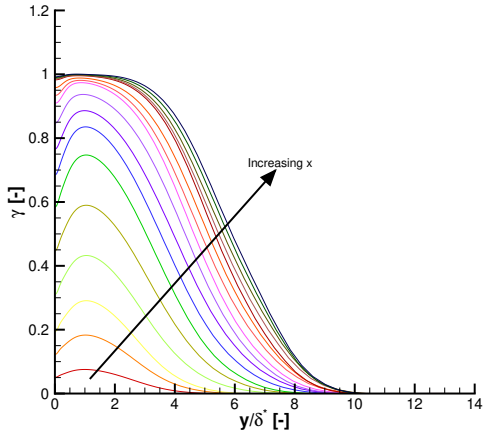

Fig. 18 Variation of γ profiles through transition.

With increasing distance away from the wall, the intermittency factor fades away, and γ is null outside of the boundary-layer. These intermittency profiles are in accordance with Sohn et al. [33] experimental profiles.

It should be noted that contrary to Menter et al. [34]'s intermittency model, γ is null outside the boundary-layer. Indeed γ does not impact the production of turbulence, but only weights on the Reynolds stress tensor in the diffusive

part of the RANS equations. Thus, turbulent features are not impacted by γ, and they can develop in the free-stream region even-though γ is null.

Figure 19 shows the familiar longitudinal distribution of γ at the wall. It also presents the skin friction coefficient during transition. The skin friction coefficient increases before transition starts. It is due to viscous-inviscid interaction

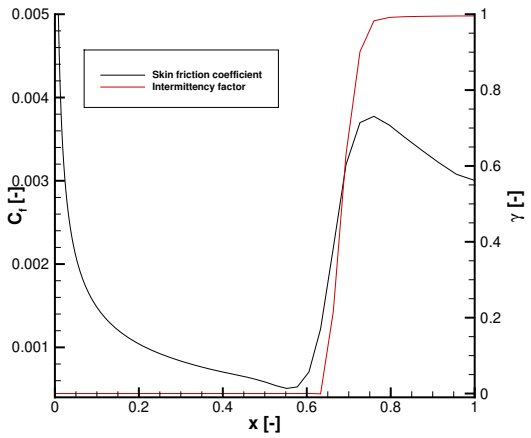

Fig. 19 Skin friction coefficient along a flat plate boundary layer undergoing transition.

that arises when intermittency is seen to behave in a point-like manner. Indeed, Stock and Haase [35] showed that point-like transition results in sharp gradients due to the sudden decrease of the displacement thickness near the onset of transition. These gradients induce important interactions between viscous and inviscid flows which have strong influence in region just upstream the transition location.

To overcome that problem, Ströer et al. [36] proposed the use of an offset length l_γ in order to shift downstream the production onset of effective eddy viscosity, and in doing so, to avoid viscous-inviscid interaction upstream the transition. The addition of such an offset will be considered in a future study.

VII. Conclusion and future work

In the present work, the Suzen and Huang intermittency model was modified to account for natural transition. A series of 37 zero pressure gradient flat-plate experiments on laminar-turbulent transition with low free-stream turbulence levels were used to develop a correlation for the spot formation and propagation parameter $\hat{n}\sigma$. The intermittency of the flow was extracted from instantaneous velocities and post-processed to account for non-constant y/δ^* measurement heights. Dhawan and Narasimha equation was fitted to the experimental intermittency, from which the spot formation and propagation parameter was obtained. It was found that $\hat{n}\sigma$ is independent of Tu for low levels of free-stream turbulence. The correlation for $\hat{n}\sigma$ was used in a modified version of Suzen and Huang intermittency model in 3C3D. Good agreements between simulation and experimental data were found. The correlation offers a simple and easy-to-implement expression of $\hat{n}\sigma$ for zero pressure gradient flows with low free-stream turbulence levels.

The intermittency model was implemented in CODA, a 3D compressible finite volume RANS solver, and coupled to Pascal et al. transported transition criteria and to the one-equation negative S-A turbulence model. The transition of a boundary-layer over a flat-plate without pressure gradient has been simulated. It was shown that these models can capture the transition onset, and produce a smooth transition from a laminar to a turbulent boundary-layer.

Futures works includes a thorough analysis of the model's behavior on industrial configurations, the consideration of the viscous/inviscid interaction at the transition onset, and the coupling of the transition and intermittency model to the $k-\omega$ SST turbulence model.

VIII. Appendix

A. Navier-Stokes equations

$$\partial_t \mathbf{u}_{ns} + \nabla \cdot \left(\mathbf{F}_c \left(\mathbf{u}_{ns} \right) - \mathbf{F}_d \left(\mathbf{u}_{ns}, \nabla \mathbf{u}_{ns} \right) \right) = 0 \tag{32}$$

where:

$$\mathbf{u}_{ns} = \begin{bmatrix} \rho \\ \rho \mathbf{v}^T \\ \rho E \end{bmatrix}; \quad \mathbf{F}_c\left(\mathbf{u}_{ns}\right) = \begin{bmatrix} \rho \mathbf{v}^T \\ \rho \mathbf{v}\mathbf{v}^T + p\mathbf{I} \\ \rho E \mathbf{v}^T + p\mathbf{v}^T \end{bmatrix}; \quad \mathbf{F}_d\left(\mathbf{u}_{ns}, \nabla \mathbf{u}_{ns}\right) = \begin{bmatrix} 0 \\ \tau \\ \mathbf{v}^T \tau + \mathbf{q}^T \end{bmatrix} \tag{33}$$

with

$$p = \left(\frac{C_p}{C_v} - 1\right)\left(\rho E - \frac{1}{2}\rho \mathbf{v} \cdot \mathbf{v}\right), \quad \tau = \left(\mu + \mu_{eff}\right)\left(\nabla \mathbf{v} + \left(\nabla \mathbf{v}\right)^T - \frac{2}{3}\left(\nabla \cdot \mathbf{v}\right)\mathbf{I}\right), \quad \mathbf{q} = -\left(\frac{\mu}{Pr} + \frac{\mu_{eff}}{Pr_t}\right) C_p \nabla \mathbf{T} \tag{34}$$

The effective turbulent viscosity μ_{eff} comes from the weighting of the turbulent eddy viscosity μ_t, given by the turbulence model by the intermittency factor: $\mu_{eff} = \gamma \mu_t$. The Prandtl number is set to $Pr = 0.72$ and the turbulent Prandtl number to $Pr_t = 0.9$. The Sutherland's law is used to give the relation between viscosity and temperature.

B. Transition Model

Pascal et al. [4] transition model accounts for natural transition induced by Tollmien-Schlichting instabilities (AHD transition criteria [37]) and by transverse transition mechanisms (C1 criterion [22]). It consists of 4 partial differential equations. The first 3 PDE transport variables needed for the AHD and C1 criteria: the critical $\widetilde{Re_\theta}$, the integral along a streamline of the Pohlhausen parameter Λ_2 and the curvilinear abscissa from the critical point $\widetilde{s_{cr}}$. The last one transports the curvilinear abscissa from the transition point $\widetilde{s_{tr}}$ needed for the intermittency model.

The transition model is defined as follow:

$$\partial_t \mathbf{u}_{tr} + \nabla\left(\mathbf{F}_c\left(\mathbf{u}_{tr}\right)\right) = \mathbf{S}\left(\mathbf{u}_{tr}, \nabla \mathbf{u}_{tr}\right) \tag{35}$$

$$\mathbf{u}_{tr} = \begin{bmatrix} \rho \widetilde{Re}_{\theta,cr} \\ \rho \widetilde{\widetilde{\Lambda}}_2 \\ \rho \widetilde{s_{cr}} \\ \rho \widetilde{s_{tr}} \end{bmatrix}; \quad \mathbf{F}_c\left(\mathbf{u}_{tr}\right) = \begin{bmatrix} b_{cr} \rho \widetilde{Re}_{\theta,cr} \mathbf{v}^T \\ \rho \widetilde{\widetilde{\Lambda}}_2 \mathbf{v}^T \\ \rho \widetilde{s_{cr}} \mathbf{v}^T \\ \rho \widetilde{s_{tr}} \mathbf{v}^T \end{bmatrix}; \quad \mathbf{S}\left(\mathbf{u}_{tr}, \nabla \mathbf{u}_{tr}\right) = \begin{bmatrix} \left(1 - b_{cr}\right)\left(\widetilde{Re}_{\theta,cr} - Re_{\theta,cr}\right) \\ b_{cr}\left(1 - b_{tr}\right)\rho \left\|\mathbf{v}\right\|_2 \Lambda_2 - \rho(1 - b_{cr})\widetilde{\widetilde{\Lambda}}_2 \\ b_{cr}\rho \left\|\mathbf{v}\right\|_2 - \rho\left(1 - b_{cr}\right)\widetilde{s_{cr}} \\ b_{tr}\rho \left\|\mathbf{v}\right\|_2 - \rho\left(1 - b_{tr}\right)\widetilde{s_{tr}} \end{bmatrix} \tag{36}$$

b_{cr} and b_{tr} are booleans. They are set to 1 where Re_θ is respectively greater than $\widetilde{Re}_{\theta,cr,e}$ and than $\widetilde{Re}_{\theta,tr}$. They are set to 0 elsewhere. Their role is to indicate if a given point along a streamline is downstream the critical point and the transition point.

C. Turbulence Model

In the CODA solver, under the RANS formulation, the negative Spalart-Allmaras turbulence model [5] reads

$$\partial_t \mathbf{u}_{turb} + \nabla \cdot \left(\mathbf{F}_c\left(\mathbf{u}_{turb}\right) - \mathbf{F}_d\left(\mathbf{u}_{turb}, \nabla \mathbf{u}_{turb}\right)\right) = \mathbf{S}\left(\mathbf{u}_{turb}, \nabla \mathbf{u}_{turb}\right) \tag{37}$$

where:

$$\begin{gathered} \mathbf{u}_{turb} = \left[\rho \widetilde{\nu}\right]; \quad \mathbf{F}_c\left(\mathbf{u}_{turb}\right) = \left[\rho \widetilde{\nu} \mathbf{v}^T\right]; \quad \mathbf{F}_d\left(\mathbf{u}_{turb}, \nabla \mathbf{u}_{turb}\right) = \left[\frac{1}{\sigma}\left(\mu + f_{n1}\rho\widetilde{\nu}\right)\nabla \widetilde{\nu}^T\right] \\ \mathbf{S}\left(\mathbf{u}_{turb}, \nabla \mathbf{u}_{turb}\right) = \left[-\rho\left(P_{\widetilde{\nu}} - D_{\widetilde{\nu}}\right) - \frac{c_{b2}}{\sigma}\rho \nabla \widetilde{\nu} + \frac{1}{\sigma}\left(\nu + f_{n1}\widetilde{\nu}\right)\nabla \rho \cdot \nabla \widetilde{\nu}\right] \end{gathered} \tag{38}$$

$P_{\widetilde{\nu}}$ and $D_{\widetilde{\nu}}$ represent the production and destruction of $\widetilde{\nu}$ and are defined as:

$$P_{\widetilde{\nu}} = \begin{cases} c_{b1}\left(1 - f_{t2}\right)\widetilde{\Omega}\widetilde{\nu} & \left(\widetilde{\nu} \geq 0\right) \\ c_{b1}\left(1 - c_{t3}\right)\widetilde{\Omega}\widetilde{\nu} & \left(\widetilde{\nu} < 0\right) \end{cases}; \quad D_{\widetilde{\nu}} = \begin{cases} \left(c_{\omega 1} f_\omega - \frac{c_{b1}}{\kappa^2} f_{t2}\right)\left(\frac{\widetilde{\nu}}{d}\right)^2 & \left(\widetilde{\nu} \geq 0\right) \\ -c_{\omega 1}\left(\frac{\widetilde{\nu}}{d}\right)^2 & \left(\widetilde{\nu} < 0\right) \end{cases} \tag{39}$$

where d is the distance to the nearest wall.

$\widetilde{\Omega}$ is the modified vorticity magnitude defined as:

$$\widetilde{\Omega} = \begin{cases} \Omega + \overline{\Omega} & \left(\overline{\Omega} \geq -c_{v2}\Omega\right) \\ \Omega + \frac{\Omega\left(c_{v2}^2\Omega + c_{v3}\overline{\Omega}\right)}{(c_{v3}-2c_{v2})\Omega - \overline{\Omega}} & \left(\overline{\Omega} < -c_{v2}\Omega\right) \end{cases}, \quad \text{with } \overline{\Omega} = \frac{\widetilde{\nu}}{(\kappa d)^2} f_{v2}, \text{ and } f_{v2} = 1 - \frac{\chi}{1 - f_{v1}} \tag{40}$$

where Ω, the magnitude of the vorticity tensor W_{ij} is written:

$$\Omega = \sqrt{2W_{ij}S_{ij}}; \quad W_{ij} = \frac{1}{2}\left(\frac{\partial u_i}{\partial x_j} + \frac{\partial u_j}{\partial x_i}\right), \tag{41}$$

The previous functions read:

$$f_{n1} = \begin{cases} 1 & (\widetilde{\nu} \geq 0) \\ \frac{c_{n1} + \chi^3}{c_{n1} - \chi^3} & (\widetilde{\nu} < 0) \end{cases}; \quad f_{t2} = c_{t3}\exp\left(-c_{t4}\chi^2\right), \quad f_\omega = g\left(\frac{1 + c_{\omega 3}^6}{g^6 + c_{\omega 3}^6}\right)^{1/6}, \tag{42}$$

with

$$g = r + c_{w2}(r^6 - r), \quad r = \min\left(r_{lim}, \frac{\widetilde{\nu}}{\Omega(\kappa d)^2}\right) \tag{43}$$

Constants in the model are: $c_{b1} = 0.1355$, $c_{b2} = 0.622$, $c_{v1} = 7.1$, $c_{v2} = 0.7$, $c_{v3} = 0.9$, $c_{w2} = 0.3$, $c_{w3} = 2.0$, $c_{t3} = 1.2$, $c_{t4} = 0.5$, $c_{n1} = 16.0$, $\sigma = 2/3$, $\kappa = 0.41$ $r_{lim} = 10$.

Solving this PDE yields $\widetilde{\nu}$ from which the turbulent eddy viscosity can be computed:

$$\mu_t = \begin{cases} \rho\widetilde{\nu} f_{v1} & (\widetilde{\nu} \geq 0) \\ 0 & (\widetilde{\nu} < 0) \end{cases}; \quad f_{v1} = \frac{\chi^3}{\chi^3 + c_{v1}^3} \quad ; \quad \chi = \frac{\widetilde{\nu}}{\nu} \tag{44}$$

D. Reconstruction of the Turbulent Kinetic Energy and its Dissipation Rate

The turbulent kinetic energy k and its dissipation rate ϵ are needed for the computation of the intermittency factor source terms (see eq. (8)). They are reconstructed from the Spalart-Allmaras turbulence model following a modified version of the Bradshaw model [38] from Rahman et al. [39].

Starting with the Bradshaw hypothesis:

$$\frac{|-\overline{uv}|}{k} = a_1 = f_{v1}\widetilde{\nu}\frac{S}{k} \tag{45}$$

The turbulence structure parameter a_1 is modified to account for near-wall variations with $a_1 = C_\mu f_{v1}^{2/3}$, which gives:

$$k = f_{v1}^{1/3}\widetilde{\nu}\frac{S}{\sqrt{C_\mu}} \tag{46}$$

S, the magnitude of the strain rate tensor is replaced by $S_k = \sqrt{\widetilde{S}^2 + S_\alpha^2}$, where $\widetilde{S}$ account for the effect of the magnitude of the vorticity tensor Ω on S and S_α is a correction that considers the mean strain rate away from the wall:

$$\widetilde{S} = f_k\left(S - \frac{|\eta| - \eta}{C_T}\right)^2, \quad S_\alpha = \frac{f_{v1}}{\kappa^2}\left(\frac{\partial\sqrt{\widetilde{\nu}}}{\partial x_i}\right)^2 \tag{47}$$

where:

$$f_k = 1 - \frac{f_{v1}}{C_T}\sqrt{\max\left(1 - \mathfrak{R}, 0\right)}; \quad \eta = S - \Omega, \quad \mathfrak{R} = |\Omega/S| \tag{48}$$

which yields:

$$k = f_{v1}^{1/3}\widetilde{\nu}\frac{S_k}{\sqrt{C_\mu}} \quad \text{and} \quad \epsilon = \sqrt{\epsilon_{wall}^2 + \widetilde{\epsilon}^2}, \quad \text{with: } \widetilde{\epsilon} = \frac{\sqrt{f_{v1}}C_\mu k^2}{\widetilde{\nu} + \nu}, \quad \epsilon_{wall} = 2C_\mu\nu S_k^2 \tag{49}$$

The constants in the model are: $C_\mu = 0.09$, $C_T = \sqrt{2}$, $\kappa = 0.41$.

References

[1] Suzen, Y., and Huang, P., "Modeling of flow transition using an intermittency transport equation," *J. Fluids Eng.*, Vol. 122, No. 2, 2000, pp. 273–284. https://doi.org/10.1115/1.4832552.

[2] Houdeville, R., "Three-dimensional boundary layer calculation by a characteristic method," *Fifth Symposium on Numerical and Physical Aspects of Aerodynamic Flows, Long Beach, January 1992*, 1992.

[3] Leicht, T., Jägersküpper, J., Vollmer, D., Schwöppe, A., Hartmann, R., Fiedler, J., and Schlauch, T., "DLR-Project Digital-X-Next Generation CFD Solver'Flucs'," *CEAS Aeronautical Journal*, 2016.

[4] Pascal, L., Delattre, G., Deniau, H., and Cliquet, J., "Stability-Based Transition Model Using Transport Equations," *AIAA Journal*, Vol. 58, No. 7, 2020, pp. 2933–2942. https://doi.org/10.2514/1.J058906.

[5] Allmaras, S. R., and Johnson, F. T., "Modifications and clarifications for the implementation of the Spalart-Allmaras turbulence model," *Seventh international conference on computational fluid dynamics (ICCFD7)*, Vol. 1902, 2012.

[6] Emmons, H. W., "The laminar-turbulent transition in a boundary layer-Part I," *Journal of the Aeronautical Sciences*, Vol. 18, No. 7, 1951, pp. 490–498. https://doi.org/10.2514/8.2010.

[7] Dhawan, S., and Narasimha, R., "Some properties of boundary layer flow during the transition from laminar to turbulent motion," *Journal of Fluid Mechanics*, Vol. 3, No. 4, 1958, pp. 418–436. https://doi.org/10.1017/S0022112058000094.

[8] Narasimha, R., "The laminar-turbulent transition zone in the boundary layer," *Progress in Aerospace Sciences*, Vol. 22, No. 1, 1985, pp. 29–80. https://doi.org/10.1016/0376-0421(85)90004-1.

[9] Arnal, D., JC, J., et al., "Etude expérimentale et théorique de la transition de la couche limite." *La Recherche Aérospatiale*, 1977.

[10] Steelant, J., and Dick, E., "Modeling of bypass transition with conditioned Navier–Stokes equations coupled to an intermittency transport equation," *International journal for numerical methods in fluids*, Vol. 23, No. 3, 1996, pp. 193–220. https://doi.org/10.1002/(SICI)1097-0363(19960815)23:3<193::AID-FLD415>3.0.CO;2-2.

[11] Cho, J. R., and Chung, M. K., "A $k-\varepsilon-\gamma$ equation turbulence model," *Journal of Fluid Mechanics*, Vol. 237, 1992, pp. 301–322. https://doi.org/10.1017/S0022112092003422.

[12] Langtry, R. B., and Menter, F. R., "Correlation-based transition modeling for unstructured parallelized computational fluid dynamics codes," *AIAA journal*, Vol. 47, No. 12, 2009, pp. 2894–2906. https://doi.org/10.2514/1.42362.

[13] Dopazo, C., "On conditioned averages for intermittent turbulent flows," *Journal of Fluid Mechanics*, Vol. 81, No. 3, 1977, pp. 433–438. https://doi.org/10.1017/S0022112077002158.

[14] Vancoillie, G., "A turbulence model for the numerical simulation of transitional boundary layers," *Laminar-Turbulent Transition*, Springer, 1985, pp. 87–92. https://doi.org/10.1007/978-3-642-82462-3_10.

[15] Simon, F. F., and Stephens, C., *Modeling of the heat transfer in bypass transitional boundary-layer flows*, Vol. 3170, National Aeronautics and Space Administration, 1991.

[16] Libby, P. A., "On the prediction of intermittent turbulent flows," *Journal of Fluid Mechanics*, Vol. 68, No. 2, 1975, pp. 273–295. https://doi.org/10.1017/S0022112075000808.

[17] Lumley, J., "Second order modeling of turbulent flows," *Von Karman Inst. for Fluid Dynamics: Prediction Methods for Turbulent Flows*, 1979.

[18] Byggstøyl, S., and Kollmann, W., "Closure model for intermittent turbulent flows," *International Journal of Heat and Mass Transfer*, Vol. 24, No. 11, 1981, pp. 1811–1822. https://doi.org/10.1016/0017-9310(81)90147-2.

[19] Savill, A., "Further progress in the turbulence modelling of by-pass transition," *Engineering Turbulence Modelling and Experiments*, Elsevier, 1993, pp. 583–592. https://doi.org/10.1016/B978-0-444-89802-9.50059-9.

[20] Mayle, R. E., "The role of laminar-turbulent transition in gas turbine engines," *Journal of turbomachinery*, 1991. https://doi.org/10.1115/1.2929223.

[21] Gostelow, J., and Walker, G., "Similarity behavior in transitional boundary layers over a range of adverse pressure gradients and turbulence levels," *Journal of turbomachinery*, 1991. https://doi.org/10.1115/1.2929125.

[22] Arnal, D., Coustols, E., and Juillen, J., "Etude expérimentale et théorique de la transition sur une aile en flèche infinie," *La Recherche Aérospatiale*, 1984, pp. 275–290. https://doi.org/10.1007/978-3-642-82462-3_69.

[23] Perraud, J., Arnal, D., Casalis, G., Archambaud, J.-P., and Donelli, R., "Automatic transition predictions using simplified methods," *AIAA journal*, Vol. 47, No. 11, 2009, pp. 2676–2684. https://doi.org/10.2514/1.42990.

[24] Schubauer, G. B., and Skramstad, H. K., "Laminar Boundary-Layer Oscillations and Transition on a flat plate," *Journal of research of the National Bureau of Standards*, Vol. 38, 1947, p. 251.

[25] Fransson, J. H., Matsubara, M., and Alfredsson, P. H., "Transition induced by free-stream turbulence," *Journal of Fluid Mechanics*, Vol. 527, 2005, pp. 1–25. https://doi.org/10.1017/S0022112004002770.

[26] Methel, J., Forte, M., Vermeersch, O., and Casalis, G., "An experimental study on the effects of two-dimensional positive surface defects on the laminar–turbulent transition of a sucked boundary layer," *Experiments in Fluids*, Vol. 60, No. 6, 2019, pp. 1–18. https://doi.org/10.1007/s00348-019-2741-2.

[27] Ducaffy, F., Forte, M., Vermeersch, O., and Piot, E., "An experimental study of the effects of surface roughness on the laminar-turbulent transition of a 2D incompressible boundary-layer," *AIAA Scitech 2021 Forum*, 2021, p. 0247. https://doi.org/10.2514/6.2021-0247.

[28] Veerasamy, D., and Atkin, C., "A rational method for determining intermittency in the transitional boundary layer," *Experiments in Fluids*, Vol. 61, No. 1, 2020, pp. 1–13. https://doi.org/10.1007/s00348-019-2856-5.

[29] Bertelrud, A., and Anders, J., "Transition Documentation on a Three-Element High-Lift Configuration at High Reynolds Numbers: Analysis," Tech. rep., NASA, 2002. https://doi.org/10.2514/6.1998-703.

[30] Matsubara, M., Alfredsson, P. H., and Westin, K. J. A., "Boundary layer transition at high levels of free stream turbulence," *Turbo Expo: Power for Land, Sea, and Air*, Vol. 78620, American Society of Mechanical Engineers, 1998, p. V001T01A063. https://doi.org/10.1115/98-GT-248.

[31] Huismann, I., Fechter, S., and Leicht, T., "HyperCODA–extension of flow solver CODA towards hypersonic flows," *STAB/DGLR Symposium*, Springer, 2020, pp. 99–109. https://doi.org/10.1007/978-3-030-79561-0_10.

[32] Spalart, P., and Allmaras, S., "A one-equation turbulence model for aerodynamic flows," *30th aerospace sciences meeting and exhibit*, 1992, p. 439. https://doi.org/10.2514/6.1992-439.

[33] Sohn, K. H., Reshotko, E., and Zaman, K. B. M. Q., "Experimental Study of Boundary Layer Transition on a Heated Flat Plate," Tech. rep., NASA, 1991.

[34] Menter, F. R., Smirnov, P. E., Liu, T., and Avancha, R., "A one-equation local correlation-based transition model," *Flow, Turbulence and Combustion*, Vol. 95, No. 4, 2015, pp. 583–619. https://doi.org/10.1007/s10494-015-9622-4.

[35] Stock, H. W., and Haase, W., "Feasibility study of e transition prediction in navier-stokes methods for airfoils," *AIAA journal*, Vol. 37, No. 10, 1999, pp. 1187–1196. https://doi.org/10.2514/2.612.

[36] Ströer, P., Krimmelbein, N., Krumbein, A., and Grabe, C., "Stability-based transition transport modeling for unstructured computational fluid dynamics including convection effects," *AIAA Journal*, Vol. 58, No. 4, 2020, pp. 1506–1517. https://doi.org/10.2514/1.J058762.

[37] Arnal, D., "Transition prediction in transonic flow," *Symposium Transsonicum III*, Springer, 1989, pp. 253–262. https://doi.org/10.1007/978-3-642-83584-1_21.

[38] Bradshaw, P., Ferriss, D., and Atwell, N., "Calculation of boundary-layer development using the turbulent energy equation," *Journal of Fluid Mechanics*, Vol. 28, No. 3, 1967, pp. 593–616. https://doi.org/10.1017/S0022112067002319.

[39] Rahman, M., Agarwal, R. K., Lampinen, M., and Siikonen, T., "Wall-distance-free version of Spalart–Allmaras turbulence model," *AIAA Journal*, Vol. 53, No. 10, 2015, pp. 3016–3027. https://doi.org/10.2514/1.J053865.